Tribological Properties of CrAlN and TiN Coatings Tested in Nano- and Micro-scale Laboratory Wear Tests

Ling Hong, Guangdong Bian, Shugen Hu, Linlin Wang, and Herbert Dacosta

We investigated the tribological properties of CrAlN and TiN coatings produced by electron beam plasma-assisted physical vapor deposition by nano- and micro-scale wear tests. For comparison, we also conducted nano-indentation, nano-scanning wear tests, and pin-on-disk tribotests on uncoated M2 steel. The results indicate that, after nano-scale sliding tests against diamond indenter and pin-on-disk tests against ceramic alumina counterface pins, the CrAlN coating presents superior abrasive wear resistance compared to the TiN-coated and uncoated M2 steel samples. Against aluminum counterface, aluminum is more prone to attach on the CrAlN coating surface compared to TiN coating, but no apparent adhesive wear was observed, which has occurred on the TiN coating.

1. Introduction

Hard coatings, from conventional TiN to a wide range of single- and multilayer coatings, such as TiCN, TiAlN, CrN, and some carbon-based coatings play an important role as surface-protective coatings for improving the lifetime and performance of cutting tools, forming dies, and some bio-components (Ref 1–8). An emerging Cr-Al-N coating (Ref 9–12) has been reported to have higher hardness, higher hardness-to-elastic modulus (H/E) ratio, exceptionally high wear resistance, and thermal stability at high temperature. Therefore, it has been considered as an advanced protective coating for cutting tools or dies. Recent work has also investigated the optical and electrical properties of CrAlN coating, and the results indicated that it can be used as a novel candidate material for high-temperature solar selective absorber coatings (Ref 13).

The pressure to reduce fuel consumption through vehicle design has been the driving force behind the development of light-weight metals and advanced high-strength steels (AHSS). Aluminum alloys, which are typically light-weight materials, have been widely employed in vehicle components and can significantly reduce their weight. On the other hand, the processing of some AHSS, such as multiphase steels, improved formability and higher strength, which allow for greater part complexity, leading to fewer individual parts, more manufacturing flexibility, and therefore weight and cost savings (Ref 14). However, to produce quality parts and to reduce repairing/maintenance time and costs of die or tools, new materials or tool coatings are needed in cutting tools and dies in order to withstand new application conditions, such as high cutting force, and compatibility with ductile counterface materials during the machining and cold-forming of light-weight metals and AHSS. The deposition and characterization of Cr-Al-N coatings have been reported in previous work (Ref 9–12). However, research on their tribological properties under various conditions such as minute load and ductile counterface materials is still desirable and needed.

In this paper, we tested the wear resistance performance of a CrAlN coating. For the purpose of comparison, the TiN-coated and uncoated samples were also tested under the same test conditions. In addition to micro-scale wear tests, such as pin-on-disk tests, nano-indentation and nano-scanning wear tests were also employed to evaluate the mechanical and tribological properties of the three samples.

2. Experimental Details

2.1 Coating Preparation

TiN and CrAlN coatings produced by the supplier (Tecvac Ltd., UK) were deposited on mirror-polished ($R_a < 0.1$ μm) and hardened M2 steel (HRC = 62-63) coupons (2.5 × 2.5 cm²). An electron beam plasma-assisted physical vapor deposition (EBPAPVD) method was adopted, which usually offers dense coatings with a good surface finish, uniform microstructure, controlled composition, tailored microstructure, and low contamination. The CrAlN coating was deposited using a twin EBPAPVD system (Tecvac IP35L), and the TiN coating was deposited using a single PAPVD system (Tecvac IP70L). During the deposition processes, bulk temperature of the substrates was monitored using a thermocouple; the deposition temperature did not exceed 500 °C.

2.2 Coating Structure Characterization

The crystalline structures of coatings were analyzed by x-ray diffraction (XRD). The thickness and surface roughness of coatings were measured by the cross-sectional morphology

Ling Hong and Shugen Hu, College of Mechanical Engineering, Zhejiang University, Hangzhou, Zhejiang 310058, People's Republic of China; Guangdong Bian and Linlin Wang, College of Engineering, Zhejiang Normal University, Jinhua, Zhejiang 321004, People's Republic of China; and Herbert Dacosta, Math, Science, and Engineering Division, Illinois Central College, 1 College Drive, East Peoria, IL 61635. Contact e-mails: hsgdj@zju.edu.cn and wanglinlin@zjnu.cn.

observation method using a scanning electron microscope (SEM) and a stylus surface roughness tester, respectively.

2.3 Laboratory Tests in Nano- and Micro-scales

A Hysitron Ub1 nano-mechanical test system was used to measure nanohardness and reduced elastic modulus (E_r) of the coated and uncoated samples at a normal load of 1000 μN. This Hysitron instrument with atomic force microscopy (AFM) functions has a two-dimensional computer-controlled piezo transducer that can perform tip sliding and scanning and simultaneously apply and monitor normal and lateral forces on the tip. The tip used is a three-sided pyramid Berkovich diamond tip with a radius of the tip curvature of ~100 nm. The same tip was also used for AFM imaging. The nano-wear resistance of the tested samples was determined by scanning nano-wear tests at a normal load of 200 μN, and the wear scanning area was 1.5×1.5 μm^2. The tip scanning velocity was set at 9 μm/s. Twenty passes of scanning were carried out on each sample. After the wear scanning, AFM functions were utilized to image the worn surfaces and determine their surface profiles. The wear rate was expressed by average wear depth per scanning pass. A nano-scratch mode was also used to determine the friction behavior during the sliding wear process with a constant normal load of 200 μN and a sliding speed of 0.25 μm/s.

To evaluate tribological properties in micro-scale, pin-on-disk (POD) tribotests were performed on the TiN- and CrAlN-coated and uncoated M2 coupons under dry sliding with a 5 N normal load, 0.1 m/s sliding speed, and 10,000 revolutions sliding distance (i.e., 150 m). The counterface pins were AA6061 aluminum and alumina balls with a diameter of 5.5 mm (Salem Specialty Ball Company). The wear track and worn counterface balls were observed using scanning electron microscopy (SEM) with energy-dispersive x-ray (EDX) analysis. A Wyko surface profilometer was used to obtain 3D images and cross-sectional profiles of the wear tracks produced. The wear loss was determined by measuring the areas of cross-sections of wear tracks, from which the wear rate k can be calculated and determined by the expression:

$$k = \frac{A \times L}{N \times l} \qquad \text{(Eq 1)}$$

where A and L are the cross-sectional area and circumference of wear track, respectively. N is the load and l is the sliding distance.

3. Results and Discussion

3.1 Coating Structure

Figure 1(a) and (b) are the XRD patterns and SEM photographs of cross-sectional structure of CrAlN and TiN coatings. The XRD test results indicate that the TiN and CrAlN coatings show phase structure of cubic TiN and CrN phase, respectively, and no hexagonal AlN phase is detected in the CrAlN coating suggesting that Al is dissolved in solid solution of CrN in the CrAlN coating. The two coatings have the same thicknesses of about 2.0 μm (Fig. 1b). The surface roughness of coatings is less than 0.1 μm. Our previous results indicated that the average atom ratios of Ti/N and Cr/Al/N in the TiN and CrAlN coatings are 50:50 and 35:15:50, respectively (Ref 15).
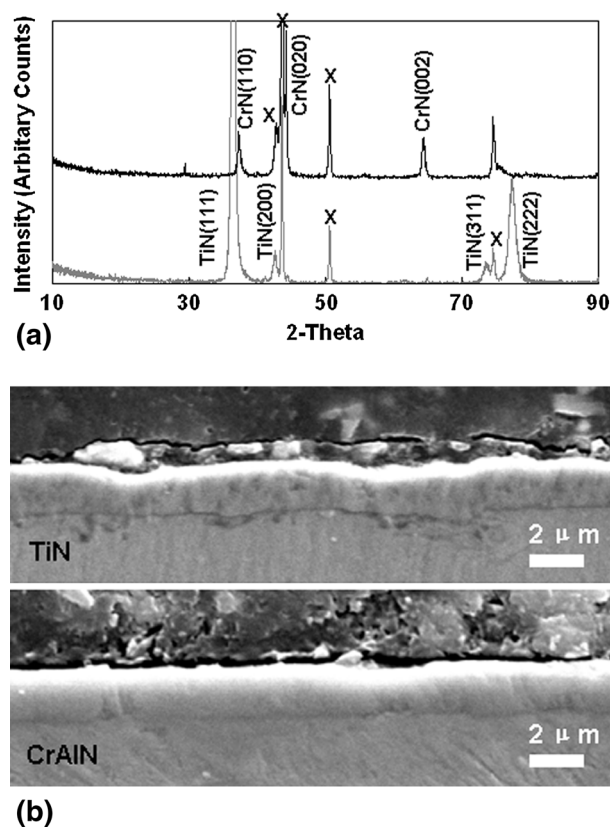

(a)

(b)

Fig. 1 (a) XRD patterns (the peaks marked with "x" are from M2 steel substrate) and (b) SEM micrographs of cross-sections of TiN and CrAlN coatings

3.2 Nano-indentation and Nano-wear

Figure 2(a) shows the load-displacement curves during the nano-indentation, and Fig. 2(b) presents the average hardness (H) and elastic modulus (E_r) determined using nano-indentation by the Oliver-Pharr method (Ref 16). Test results are also summarized in Table 1. The CrAlN coating exhibited the highest hardness, about 31.5 GPa, which is about 4 times higher than that of the uncoated M2 steel (8.6 GPa). TiN had a hardness of 25.2 GPa. While the elastic modulus of the uncoated M2 steel was 210 GPa, CrAlN and TiN coatings had similar elastic modulus values ~260 GPa. It was found that the CrAlN coating has the highest H/E_r value which often indicates that the coating would have a better wear resistance than the others (Ref 17).

Figure 3 shows 3D images of nano-wear scars. A large amount of deformation and pile-up phenomena can be observed on M2 worn surface (Fig. 3a). Figure 3(b, c) shows the uniform material removal in the wear scars of TiN and CrAlN coatings, respectively, of which the coating materials were worn away without large deformation. The nano-wear rates in unit of depth per pass were also listed in Table 1. The wear rates of uncoated M2 steel, TiN, and CrAlN are 0.93, 0.31, and 0.045 nm/pass, respectively. These results indicated that CrAlN coating could improve the wear resistance of M2 steel substrate by about 20 times, and it had an anti-wear performance of about 3 times better than the TiN coating.

The coefficient of friction (C.O.F) during nano-scratch tests was recorded and is shown in Fig. 4(a). The average values
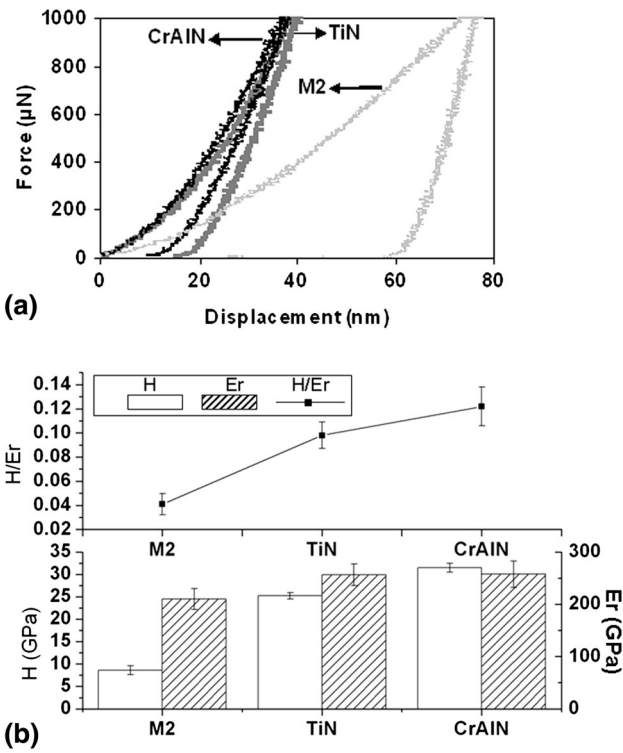
Fig. 2 (a) Load-displacement curves (b) hardness (*H*), reduced elastic modula (*E*$_r$), and *H*/*E*$_r$

Table 1 Mechanical and tribological properties of samples tested by a nano-mechanical test system

	M2	**TiN**	**CrAlN**
H, GPa	8.6 ± 0.3	25.2 ± 0.5	31.5 ± 0.4
E$_r$, GPa	209.8 ± 20	256.2 ± 20.0	257.5 ± 30.0
H/*E*$_r$	0.041	0.098	0.116
Average C.O.F (nano-scratch)	0.28-0.34	0.15	0.12
Wear rate (nm/pass)	0.93	0.31	0.045

were included in Table 1. Figure 4(b) is the magnified C.O.F curve during 1 μm sliding distance to present details of wear behaviors. Figure 4(c) is the surface profiles before nano-scratches. The C.O.F curves of all specimens exhibited a wavelike behavior. The C.O.F of M2 steel (Fig. 4a) increased to 0.34 in a fluctuated pattern. CrAlN coating exhibited a lower average friction coefficient (0.12) than TiN (0.15).

From the C.O.F curve (Fig. 4a) and wear scar image (Fig. 3a) of M2 steel, it can be inferred that nano-scale plowing has occurred under the constant normal load of 200 μN. The friction coefficient fluctuated with sliding distance (shown in Fig. 4a), which is possibly due to complicated deformation, debris formation, adhesion, and rupture. During the nano-scale wear tests on the coated samples, the diamond tip abraded the hard coatings. Thus, the two coatings have similar C.O.Fs due to the similar wear mechanisms during the nano-wear tests. Comparing the C.O.F graphs (Fig. 4b) and corresponding surface profiles (Fig. 4c) of TiN and CrAlN, it was noticed that the change trend of C.O.F agrees with the morphology of the surface profiles which is associated with the size of the asperities on the coating surface. This phenomenon can be
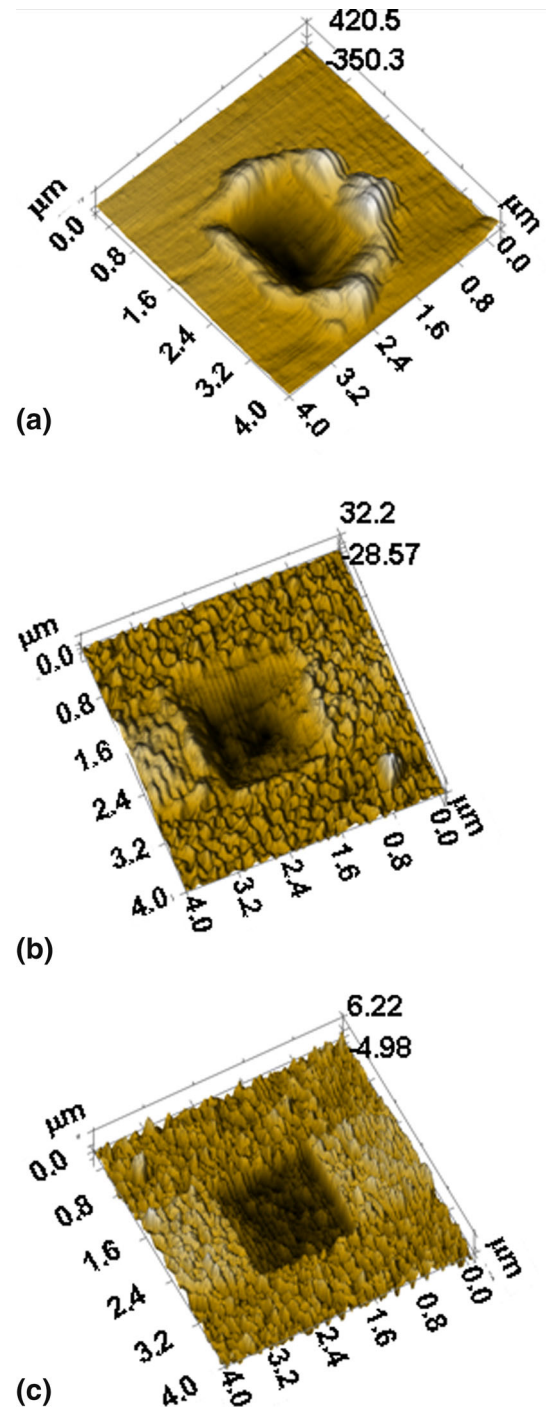

Fig. 3 3D images of nano-wear scars on (a) M2 steel and (b) TiN and (c) CrAlN coatings after 20 scanning wear passes

explained by the 'ratchet' mechanism proposed by Bhushan and co-workers (Ref 18, 19). If an angle θ relative to the horizontal plane is formed when a small tip slides over an asperity, the measured instantaneous coefficient of friction μ$_1$ in the ascending part is described by

$$\mu_1 = \mu_0 + \tan\theta \qquad (Eq\ 2)$$

Similarly, the measured instantaneous coefficient of friction μ$_2$ on the descending part of the asperity is expressed by
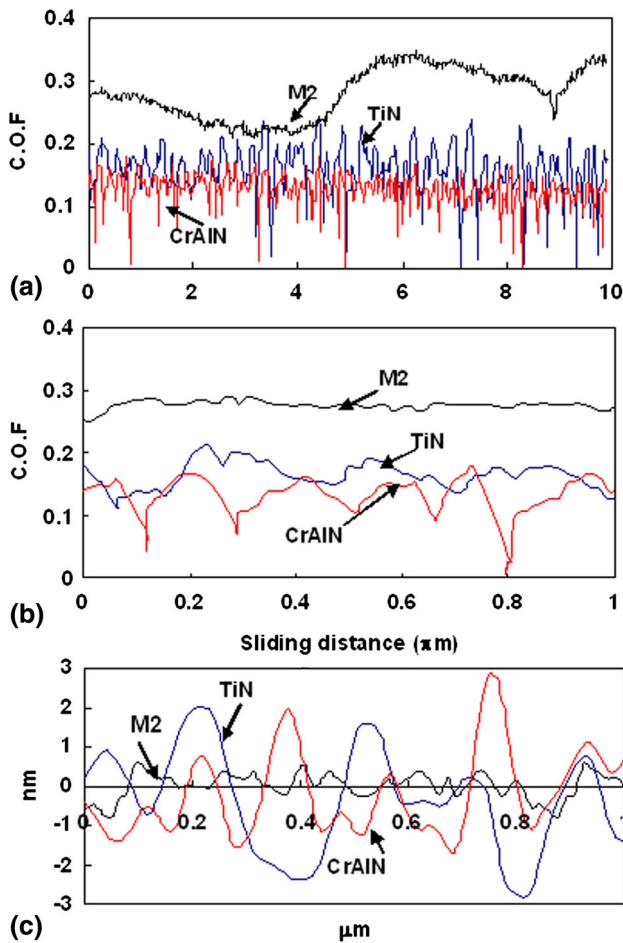
Fig. 4 (a) Coefficient of friction (C.O.F) during the nano-scratch, (b) magnified graphs during 1 μm sliding distance, and (c) surface profile before wear tests by AFM

$$\mu_2 = \mu_0 - \tan\theta \qquad (Eq\ 3)$$

where μ_0 is the constant value of the coefficient of friction for small θ. Thus, the measured friction is high at the leading edge of asperities and low at the trailing edge. The C.O.F evolution would result from friction changing correspondence to surface profiles of the hard coatings.

3.3 Micro-wear Properties

The abrasive wear resistance of coatings was evaluated by the sliding tests against hard alumina pins/balls. Figure 5 shows the wear behavior for the M2 steel and the coatings using alumina pins as the counterface. The achieved average C.O.F values were listed in Table 2. The CrAlN coating has lower C.O.F (about 0.55) than the TiN coating (~0.8), and the M2 has a C.O.F of about 0.8. Figure 6(a, c, e) shows the SEM micrographs of wear tracks against alumina counterface balls, and their corresponding magnified images are shown in Figure 6(b, d, f), respectively. On the wear tracks of M2 steel (Figure 6a, b) and TiN coating (Figure 6c, d), severe abrasive wear can be observed. In addition, a number of white spots can
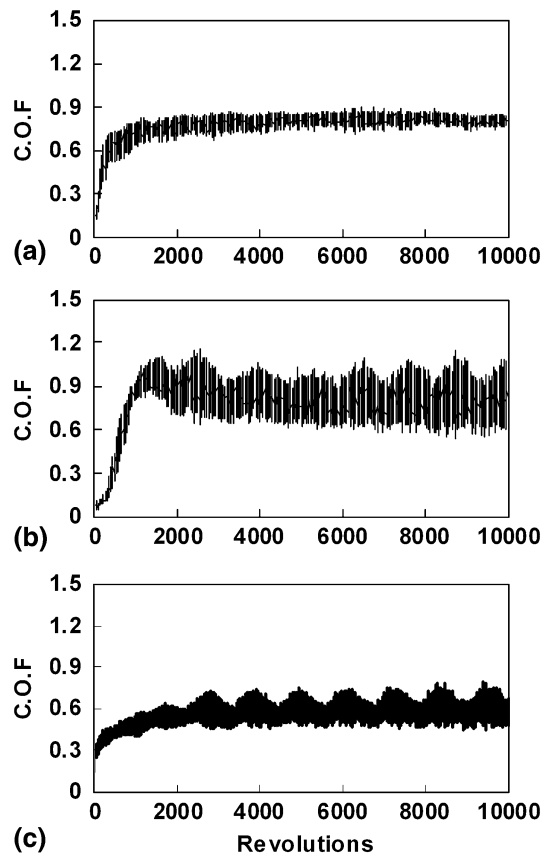

Fig. 5 Coefficient of friction (C.O.F) during pin-on-disk sliding tests on (a) uncoated M2 steel and coatings of (b) TiN and (c) CrAlN vs. alumina pins

Table 2 Tribological properties tested by pin-on-disk sliding wear tests

	M2	TiN	CrAlN
C.O.F (pin-on-disk)			
vs. Al pin	0.64	0.54	0.67
vs. Al_2O_3 pin	0.81	0.80	0.55
Wear rate, μm^3/N m			
vs. Al_2O_3 pin	5.02	3.40	Negligible
Al ball wear loss (μm^3)	2.32×10^5	2.58×10^6	5.04×10^6

be observed at the local areas on the wear track of TiN coating (Fig. 6d). The EDX analysis showed that the white areas contain the elements W, Mo, Ti, V, and Cr, similar to the composition of M2 substrate, indicating that the TiN coating had been locally penetrated at the center area of the wear track. Some golden color TiN particles were also found on the alumina ball from the SEM observation (shown in the inset of Fig. 6c). For CrAlN coating, no obvious wear but only polishing and one non-continuous scratching scar were observed in the wear track (Fig. 6e, f), and little wear occurred on the counterface ceramic ball. A large amount of plastic deformation and two-body abrasive wear occurred where hard ceramic ball grinded the M2 steel surface and the ceramic ball
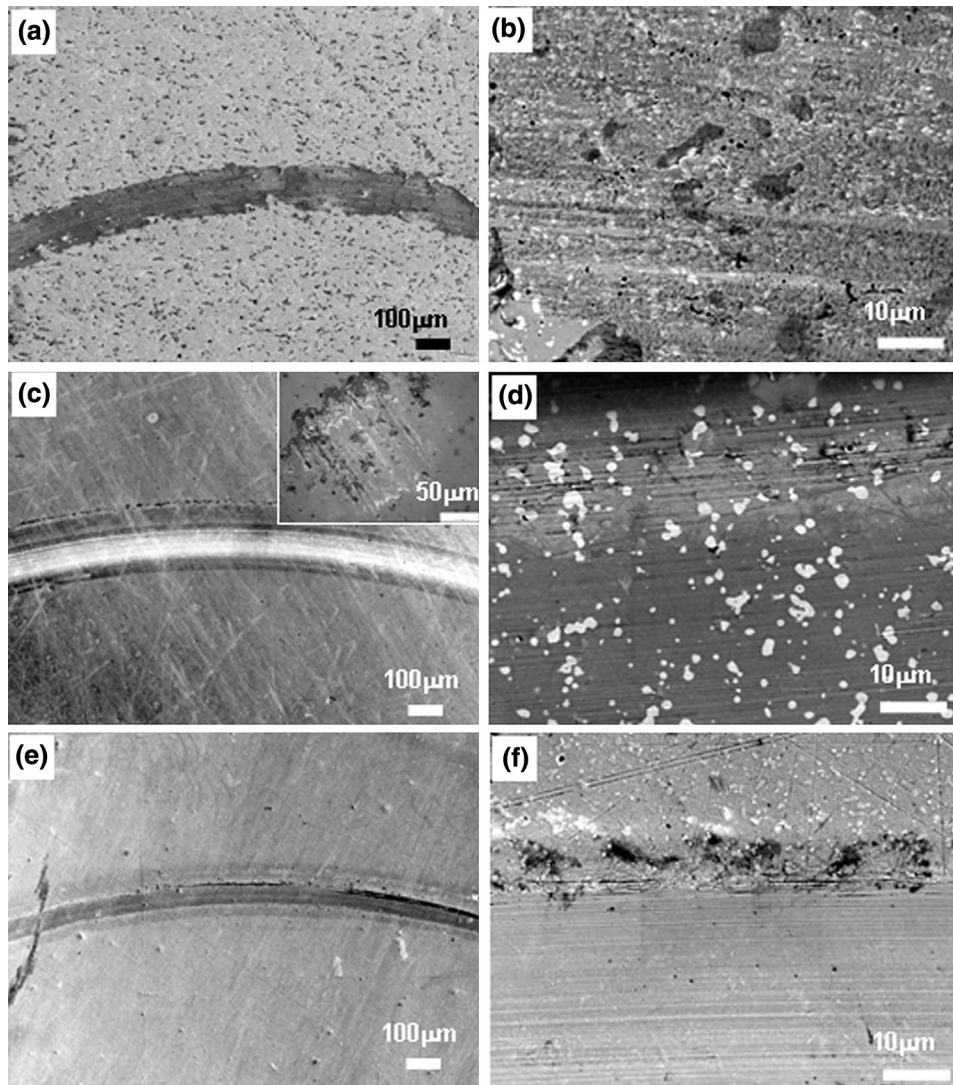
Fig. 6 SEM micrographs of the wear tracks after pin-on-disk tests against alumina pin balls on (a) uncoated M2 steel, (c) TiN with inset showing the alumina counterface pin, (e) CrAlN, and (b, d, f) are the corresponding high-magnification micrographs

was not worn. While, for the TiN coating, the ceramic ball abraded the TiN coating and some wear debris served as "third body," and therefore more severe abrasive wear occurred on the TiN coating surface which causes the higher C.O.F of TiN coating than the CrAlN coating. The similar values of TiN and uncoated M2 steel could coincide.

The wear rates of the three samples against alumina balls are listed in Table 2. From the results, it can be found that the wear resistance of TiN is 1.5 times higher than that of uncoated M2 steel, and wear loss on CrAlN coating is negligible. The order of wear resistance during pin-on-disk tests against alumina pins is consistent with that in nano-wear tests.

Figure 7 shows the C.O.F of M2 steel and TiN and CrAlN coatings when sliding against aluminum pins. The obtained average C.O.Fs are listed in Table 2. During a running-in process, C.O.Fs of M2 steel and CrAlN coating increased gradually, and then the C.O.Fs stabilized at an average value of

0.64 and 0.67, respectively, while TiN exhibited the lowest C.O.F of 0.54 among the three samples. Figure 8(a, b, c) shows the SEM micrographs of wear tracks on the M2 steel and TiN and CrAlN coatings after sliding tests against aluminum counterface balls. Figure 8(d, e, f) shows the 3D images of wear tracks and corresponding 2D profiles of cross-sectional wear tracks. The wear track on the uncoated M2 steel (Figure 8a, d) exhibited severe adhesive and abrasive wear. The M2 material was sheared away by the effect of adhesion junctions. Meanwhile, the wear debris serves as the third body between counterfaces and then leads to the abrasive wear. For TiN (Fig. 8b, e) and CrAlN (Fig. 8c, f) coatings, large amounts of material transferring from the aluminum balls to the wear tracks can be observed. The transferred aluminum material covered the surface of wear tracks. On the TiN coating, some coating chipping can be observed which implied that some adhesive wear had occurred on the coating surface. For the
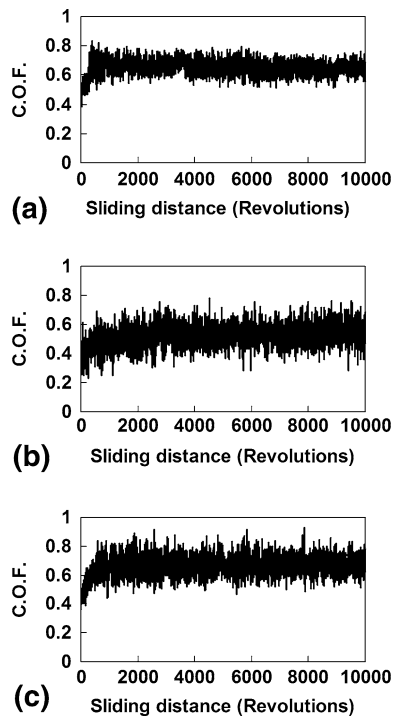
Fig. 7 Coefficient of friction (C.O.F) during pin-on-disk sliding tests on (a) uncoated M2 steel and coatings of (b) TiN and (c) CrAlN vs. aluminum pins

CrAlN coating, more significant material transferring but no coating chipping can be observed in the wear tracks. At the steady stage of the sliding, the aluminum materials attached on the samples' surface and formed transferred layers. Under such circumstance, the real contact surfaces are transferred aluminum layer and the worn aluminum balls. Thus, the uncoated M2 sample has a similar C.O.F value as the CrAlN coating. The reason of lower C.O.F of TiN coating could be due to less material transferring on TiN coating and lower junction strength between aluminum and the TiN compared to the CrAlN coating.

Similar wear resistance results have been reported in a previous work (Ref 15), where the TiN and CrAlN coatings have been applied on punches in an industrial stamping die. The CrAlN-coated punch has a longer lifetime than TiN-coated and uncoated punches when stamping the hot-dip zinc high-strength steel sheets. The SEM images of the counterface aluminum balls (photographs did not present here) show that all the balls were worn and little material attached on their surfaces, but some abrasive wear can still be observed on the surfaces of all balls. The calculated wear loss of the aluminum balls against different

counterfaces is shown in Table 2. The wear loss against the three samples is in the order CrAlN > TiN > M2 steel. The above results indicate that CrAlN coating has higher affinity to Al counterface material compared to TiN coating and M2 steel. The XRD pattern of CrAlN shows that Al is dissolved in solid solution of CrN rather than forming AlN, and the Al in the crystalline could form Al-Al bond with the Al counterface which accounts for the increase of the affinity between CrAlN and aluminum. No obvious adhesive wear occurred, which is due to the high wear resistance of CrAlN coating. However, large amounts of Al sticking could lead to built-up edge on the cutting tool which has negative effects on the cutting quality.

The comparative results showed that the nano-scaled wear tests against a diamond indenter and micro-scaled wear tests against alumina ceramic counterface balls presented a similar trend in ranking of wear resistance. Thus, nano-wear tests can be used to predict the wear resistance of hard coatings under micro-scale wear test when abrasive wear mechanism is the predominated wear mechanism for both scale tests. However, when complicated plastic deformation, adhesion, and tribo-chemical reaction occurred during the micro-scaled sliding tests against aluminum balls, the wear mechanism of micro-scaled wear test is different from that of nano-scaled one. Under the aforementioned conditions, it is not suitable to use nano-scaled results to evaluate the coating's wear resistance under the micro-scale wear test.

4. Conclusions

In nano-scale tests, CrAlN coating exhibited higher hardness (H) and H/E ratio as well as lower friction coefficient compared with TiN coating and uncoated hardened M2 steel. The wear resistance of the CrAlN coating was 20 times higher than that of M2 steel and about 3 times higher than that of the TiN coating.

When sliding against ceramic alumina balls during micro-scale pin-on-disk tests, the wear mechanism is dominantly abrasive wear. The CrAlN coating presents the best wear resistance, lowest C.O.F, and negligible wear loss after sliding tests, whereas TiN coating was penetrated due to the severe abrasive wear. The trend of wear resistance among the three samples is consistent with that in nano-scale test.

When sliding against aluminum pins, more materials are transferred from aluminum balls to coating CrAlN, compared with uncoated and TiN-coated M2 steel, but coating wear did not occur in the CrAlN coating during the pin-on-disk sliding tests. The laboratory nano- and micro-scale tests showed that the CrAlN coating had higher wear resistance than the TiN coating and uncoated M2 steel.
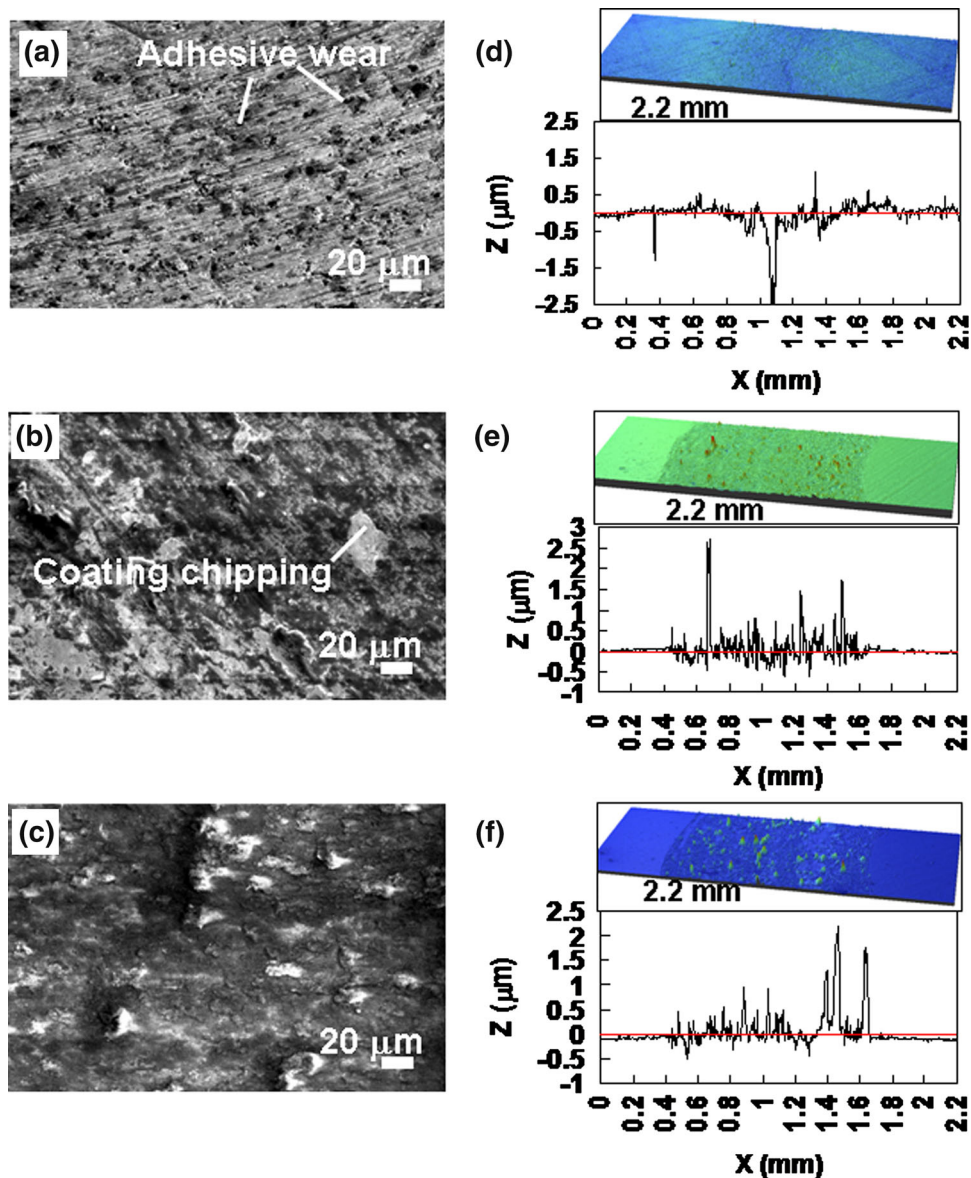
Fig. 8 (a, b, c) SEM micrographs of the wear tracks after pin-on-disk test against aluminum pin balls; (d, e, f) 3D images of wear tracks and 2D profiles of cross-sections of wear tracks on (a, d) uncoated, (b, e) TiN-coated, and (c, f) CrAlN-coated M2 steel

References

1. H.A. Ching, D. Choudhury, M.J. Nine, and N.A. Abu Osman, Effects of Surface Coating on Reducing Friction and Wear of Orthopaedic Implants, *Sci. Technol. Adv. Mater*, 2014, **15**, p 1–21
2. K.V. Chauhan and S.K. Rawal, A Review Paper on Tribological and Mechanical Properties of Ternary Nitride based Coatings, *Procedia Technol.*, 2014, **14**, p 430–437
3. E.E. Vera, M. Vite, R. Lewis, E.A. Gallardo, and J.R. Laguna-Camacho, A Study of the Wear Performance of TiN, CrN and WC/C Coatings on Different Steel Substrates, *Wear*, 2011, **271**, p 2116–2124
4. B. Subramanian, R. Ananthakumar, and M. Jayachandran, Structural and Tribological Properties of DC Reactive Magnetron Sputtered Titanium/Titanium Nitride (Ti/TiN) Multilayered Coatings, *Surf. Coat. Technol.*, 2011, **205**, p 3485–3492
5. L. Cunha, M. Andritschky, K. Pischow, Z. Wang, A. Zarychta, A.S. Miranda, and A.M. Cunha, Performance of Chromium Nitride and Titanium Nitride Coatings During Plastic Injection Moulding, *Surf. Coat. Technol.*, 2002, **153**, p 160–165
6. A. Lousa, J. Romero, E. Martínez, J. Esteve, F. Montalà, and L. Carreras, Multilayered Chromium/Chromium Nitride Coatings for Use in Pressure Die-Casting, *Surf. Coat. Technol.*, 2001, **146-147**, p 268–273
7. L. Wang, X. Nie, M.J. Lukitsch, J.C. Jiang, and Y.T. Cheng, Effect of Tribological Media on Tribological Properties of Multilayer Cr(N)/C(DLC) Coatings, *Surf. Coat. Technol.*, 2006, **201**, p 4341–4347
8. P. Zhang, L. Wang, and X. Nie, Tribological Properties of a-C/Cr(N) Coatings in Micro- and Nano-Scales, *Surf. Coat. Technol.*, 2007, **201**, p 5176–5181
9. L. Wang and X. Nie, Effect of Annealing Temperature on Tribological Properties and Material Transfer Phenomena of CrN and CrAlN Coatings, *J. Mater. Eng. Perform.*, 2014, **23**, p 560–571

10. X.-Z. Ding, A.L.K. Tan, X.T. Zeng, C. Wang, T. Yue, and C.Q. Sun, Corrosion Resistance of CrAlN and TiAlN Coatings Deposited by Lateral Rotating Cathode Arc, *Thin Solid Films*, 2008, **516**, p 5716–5720

11. S. Yang, K. Cooke, H. Sun, X. Li, K. Lin, and H. Dong, Development of Advanced Duplex Surface Systems by Combining CrAlN Multilayer Coatings with Plasma Nitrided Steel Substrates, *Surf. Coat. Technol.*, 2013, **236**, p 2–7

12. L. Aihua, D. Jianxin, C. Haibing, C. Yangyang, and Z. Jun, Friction and Wear Properties of TiN, TiAlN, AlTiN and CrAlN PVD Nitride Coatings, *Int. J. Refract. Met. Hard Mater.*, 2012, **31**, p 82–88

13. J. Chen, C. Guo, J. Chen, J. He, Y. Ren, and L. Hu, Microstructure, Optical and Electrical Properties of CrAlN Film as a Novel Material for High Temperature Solar Selective Absorber Applications, *Mater. Lett.*, 2014, **133**, p 71–74

14. J. Galan, L. Samek, P. Verleysen, K. Verbeken, and Y. Houbaert, Advanced High Strength Steels for Automotive Industry, *Rev. Metal.*, 2012, **48**, p 118–131

15. L. Wang, X. Nie, J. Housden, E. Spain, J.C. Jiang, E.I. Meletis, A. Leyland, and A. Matthews, Material Transfer Phenomena and Failure Mechanisms of a Nanostructured Cr-Al-N Coating in Laboratory Wear Tests and an Industrial Punch Tool Application, *Surf. Coat. Technol.*, 2008, **203**, p 816–821

16. W.C. Oliver and G.M. Pharr, An Improved Technique for Determining Hardness and Elastic-Modulus Using Load and Displacement Sensing Indentation Experiments, *J. Mater. Res.*, 1992, **7**, p 1564–1583

17. A. Leyland and A. Matthews, On the Significance of the H/E Ratio in Wear Control: A Nanocomposite Coating Approach to Optimised Tribological Behaviour, *Wear*, 2000, **246**, p 1–11

18. N.S. Tambe and B. Bhushan, Scale Dependence of Micro/Nano-friction and Adhesion of MEMS/NEMS Materials, Coatings and Lubricants, *Nanotechnology*, 2004, **15**, p 1561–1570

19. C.K. Ng, S.N. Melkote, M. Rahman, and A. SenthilKumar, Experimental Study of Micro- and Nano-scale Cutting of Aluminum 7075-T6, *Int. J. Mach. Tools Manuf.*, 2006, **46**, p 929–936